11-6-2015

Antioncogenic and Oncogenic Properties of Nrf2 in Arsenic-Induced Carcinogenesis

Young-Ok Son
University of Kentucky, young-ok.son@uky.edu

Poyil Pratheeshkumar
University of Kentucky, pratheeshkumar.poyil@uky.edu

Ram Vinod Roy
University of Kentucky

Andrew Hitron
University of Kentucky, a.hitron@uky.edu

Lei Wang
University of Kentucky, lei.wang1@uky.edu

See next page for additional authors

Right click to open a feedback form in a new tab to let us know how this document benefits you.

Follow this and additional works at: https://uknowledge.uky.edu/environmental_disease_facpub

Part of the Disorders of Environmental Origin Commons

Authors

Young-Ok Son, Poyil Pratheeshkumar, Ram Vinod Roy, Andrew Hitron, Lei Wang, Sasidharan Padmaja Divya, Mei Xu, Jia Luo, Gang Chen, Zhuo Zhang, and Xianglin Shi

Antioncogenic and Oncogenic Properties of Nrf2 in Arsenic-Induced Carcinogenesis

Antioncogenic and Oncogenic Properties of Nrf2 in Arsenic-induced Carcinogenesis*

Young-Ok Son[‡§1,2], **Poyil Pratheeshkumar**[‡§1], **Ram Vinod Roy**[‡§], **John Andrew Hitron**[§], **Lei Wang**[‡§], **Sasidharan Padmaja Divya**[§], **Mei Xu**[¶], **Jia Luo**[¶], **Gang Chen**[¶], **Zhuo Zhang**[§], and **Xianglin Shi**[‡§3]

From the ‡Center for Research on Environmental Disease and Departments of §Toxicology and Cancer Biology and ¶Pharmacology and Nutritional Sciences, College of Medicine, University of Kentucky, Lexington, Kentucky 40536-0305

Background: Arsenic induced cell transformation and carcinogenesis.
Results: Arsenic-transformed cells have the property of apoptosis/autophagy resistance.
Conclusion: The constitutive activation of Nrf2 in arsenic-transformed cells up-regulates antioxidants, decreases ROS generation, and causes apoptosis resistance and tumorigenesis.
Significance: Antioncogenic role of inducible Nrf2 in normal cells and oncogenic role of constitutive activation of Nfr2 in cancer cells may increase our understanding of the mechanism of arsenic carcinogenesis and its prevention.

Arsenic (As^{3+}) is a carcinogen with considerable environmental and occupational relevancy. The present study shows that As^{3+}-transformed human lung bronchial epithelial BEAS-2B cells (AsT cells) exhibit the property of apoptosis resistance. The level of basal reactive oxygen species (ROS) is very low in AsT cells in correlation with elevated expressions of both antioxidant enzymes and antiapoptotic proteins. Nuclear factor erythroid 2-related factor (Nrf2) and p62 are constitutively expressed. These two proteins up-regulate antioxidant enzymes and antiapoptotic proteins. The knockdown of Nrf2 or p62 by small interfering RNA (siRNA) enhanced both ROS levels and As^{3+}-induced apoptosis in transformed cells. AsT cells have autophagy deficiency as evidenced by reduced formation of microtubule-associated protein 1 light chain 3 (LC3)-II, GFP-LC3 puncta, and autophagy flux. Results obtained using a soft agar assay and shRNA Nrf2-transfected cells show that Nrf2 plays an antioncogenic role before transformation, whereas this transcription factor plays an oncogenic role after transformation. In addition, depletion of Nrf2 by shRNA dramatically inhibited growth and proliferation of transformed cells. Furthermore, the Nrf2 protein levels and antiapoptotic and antioxidant enzyme levels are higher in lung adenocarcinoma than in normal tissues. Collectively, this study demonstrates that a constitutively high level of Nrf2 in AsT cells up-regulates the antioxidant proteins catalase and superoxide dismutase as well as the antiapoptotic proteins Bcl-2 and Bcl-xL. The final consequences are decreased ROS generation and increased apoptotic resistance, cell survival and proliferation, and tumorigenesis.

The nuclear factor erythroid 2-related factor (Nrf2)[4] is a master regulator of cellular antioxidant responses. Under unstressed conditions, Nrf2 is degraded by proteasomal machinery. However, under oxidative stress condition, Nrf2 translocates to the nucleus and activates antioxidant proteins and detoxification enzymes (1). The p62/sequestosome 1 protein is a multifunction, ubiquitin-binding adapter protein that serves multiple cellular functions for autophagy, apoptosis, reactive oxygen species (ROS) signaling, and cancer development (2, 3). The accumulated p62 competitively binds to the Nrf2-binding site of Keap1 and promotes the constitutive activation of Nrf2 transcriptional programs (4). Thus, p62 accumulation activates Nrf2 and Nrf2 target gene expression (5, 6).

In general, apoptosis serves as a natural barrier to tumor development (7). The apoptotic machinery is controlled by pro- and antiapoptotic members of the Bcl-2 family (7). Cancer cells have a variety of strategies to escape apoptosis such as the loss of the p53 tumor suppressor and an increase in expression of antiapoptotic proteins such as Bcl-2 and Bcl-xL (8, 9).

Autophagy is thought to play a dual role in carcinogenesis. For example, autophagy helps tumor growth, metabolism, and survival via nutrient recycling (10). However, autophagy can prevent tumor initiation by suppressing inflammation, tissue damage, and genomic instability through its quality control function (11).

It has been reported that inducible Nrf2 activation reduces carcinogenesis, especially in its early stages (12–14). It has been shown that inducible Nrf2 activation is important in the anticancer effects of many natural compounds, including phenethyl isothiocyanate, curcumin, and resveratrol (12). However,

---

---

a constitutively high level of Nrf2 protects cancer cells against oxidative stress and chemotherapeutic agents (15). The antioncogenic or oncogenic role of Nrf2 may depend on the stage of carcinogenesis. Nrf2 activity may be desirable in early stages of carcinogenesis when the host is seeking to control premalignant carcinogenesis, but constitutive Nrf2 activation may be undesirable in later stages when it may induce resistance to apoptosis in malignant cancer cells. Despite recent advances in understanding the mechanism of As^{3+}-induced Nrf2 activation, the role of Nrf2 in As^{3+}-induced carcinogenesis (protection against or promotion of carcinogenesis) remains unexplored. The central hypothesis is that Nrf2 is antioncogenic in early stages of As^{3+}-induced carcinogenesis (cell transformation) by an up-regulation of antioxidants to reduce As^{3+}-induced ROS; however, once a cell is transformed, Nrf2 is oncogenic by inducing apoptosis resistance. This study also will examine how constitutive activation of Nrf2 contributes to apoptosis resistance as well as a decrease in ROS generation and tumorigenesis in transformed cells.

Materials and Methods

Cell Culture and Treatment—The human lung bronchial epithelial cell line BEAS-2B was obtained from the American Type Culture Collection (Manassas, VA). As^{3+}-transformed cells were generated as described previously (16). The transformation ability and tumorigenicity of the transformed cells were confirmed by soft agar assay and xenograft assay, respectively.

Plasmids and Transfection—The overexpression of catalase, SOD1, and SOD2 in BEAS-2B cells has been described previously (17). The mCherry-EGFP-LC3B plasmid was purchased from Addgene (Cambridge, MA), and GFP-LC3 plasmid has been described previously (18). shRNAs for knockdown of catalase and SOD2 were obtained from (OriGene Technologies, Inc., Rockville, MD). Transfections were performed using Lipofectamine™ 2000 (Invitrogen) according to the manufacturer's protocol.

Nrf2 and p62 Knockdown—Silencer predesigned siRNAs for human p62 (siRNA ID s16960) and Nrf2 (siRNA ID s9491) and control siRNA (AM4611) were obtained from Ambion (Austin, TX). Four unique human 29-mer shRNA constructs in retroviral GFP vector for Nrf2 (TG311194) and p62 (TG309121) were purchased from OriGene Technologies, Inc.

Chromatin Immunoprecipitation (ChIP) Assay—A ChIP assay was performed using a Pierce™ Agarose ChIP kit (Thermo Scientific, Rockford, IL). Sheared chromatin was diluted and immunoprecipitated with 2 μg of anti-Nrf2 or control IgG antibody. DNA-protein complexes were eluted from the protein A/G-agarose beads using a spin column and reverse cross-linked by incubating with NaCl at 65 °C. The relative Nrf2 binding to the ARE regions of p62, Bcl-2, and Bcl-xL was analyzed by the MyiQ™ Single-Color Real-Time PCR Detection System (Bio-Rad) with SYBR Green PCR Master Mix. General PCR amplification was also performed using Mastercycler® thermal cyclers (Eppendorf, Foster City, CA).

Human Tissue Samples—Human lung adenocarcinoma tissue (stage IA or IIA) was provided from the Biospecimen and Tissue Procurement Shared Resource Facility of the University of Kentucky Markey Cancer Center. Frozen lung cancer tissues

were homogenized with MagNA Lyser Green Beads using a MagNA Lyser instrument (Roche Applied Science), and Western blotting analysis was performed.

Immunohistochemical Staining—Tumor tissues were fixed with 4% paraformaldehyde at room temperature for 24 h, embedded in paraffin, and sectioned (3–4-μm thickness). The slides were deparaffinized, rehydrated, and processed for immunohistochemical staining according to the VECTASTAIN ABC kit protocol (Vector Laboratories, Burlingame, CA).

Statistical Analysis—All the data are expressed as means $\pm$ S.E. One-way analysis of variance (ANOVA) using IBM SPSS Statistics 21 was used for the multiple comparisons. A value of $p < 0.05$ was considered statistically significant.

Results

As^{3+}-transformed BEAS-2B Cells Have the Property of Cell Death Resistance—Arsenic-induced transformed BEAS-2B cells (AsT cells) showed less cell death when these cells were exposed to As^{3+} compared with non-transformed cells (Fig. 1, *A–C*). The AsT cells had a higher proliferative potential and colony forming ability than the non-transformed BEAS-2B cells (Fig. 1, *D* and *E*). Approximately 30% of cell populations were apoptotic in the As^{3+}-exposed normal cells. However, apoptosis occurred only in a few cell populations in AsT cells (Fig. 1, *F* and *G*). The cleaved poly(ADP-ribose) polymerase and caspase-3/7 expression was dose-dependent in the non-transformed cells but not in AsT cells (Fig. 1*H*). Further study revealed that As^{3+}-induced cell death occurred mainly through caspase-dependent apoptosis (Fig. *I*).

A Low Level of ROS Is Caused by High Expressions of Antioxidant Enzymes, and High Expressions of Bcl-2 and Bcl-xL Are Involved in Cell Death Resistance Mechanisms of AsT Cells—Electron spin resonance (ESR) measurements show that the normal BEAS-2B cells generated a high 1:2:2:1 quartet signal indicative of ROS generation and that the signal was very low in the AsT cells (Fig. 2*A*). Furthermore, we stained the cells with 5-(and-6)-chloromethyl-2′,7′-dichlorodihydrofluorescein diacetate to measure intracellular ROS levels and analyzed fluorescence intensity using flow cytometry (Fig. 2*B*), fluorescence microscopy (Fig. 2*C*), and a fluorescence microplate reader (Fig. 2*D*). The expressions of catalase and superoxide dismutase 2 were much higher in AsT cells than in non-transformed parent cells (Fig. 2*E*). When the cells were exposed to As^{3+}, the expressions of antioxidant enzymes were reduced in a dose-dependent manner in normal BEAS-2B cells, whereas the levels of antioxidant enzymes were only slightly decreased upon exposure to As^{3+} at 20 μM in the AsT cells (Fig. 2*F*). The knockdown of these antioxidant enzymes by shRNA transfection in the AsT cells restored the levels of ROS (Fig. 2*G*). The basal levels of Bcl-2 and Bcl-xL were higher in the AsT cells than in the non-transformed cells (Fig. 2*H*). The decrease in the levels of Bcl-2 and Bcl-xL by As^{3+} was much lesser in AsT cells in a dose- and time course-dependent manner (Fig. 2, *I* and *J*). Depletions of Bcl-2 and Bcl-xL expressions by adding ABT-263, a Bcl-2 family inhibitor, resulted in complete inhibition of Bcl-2 and Bcl-xL expressions (Fig. 2*K*). The viability of As^{3+}-exposed
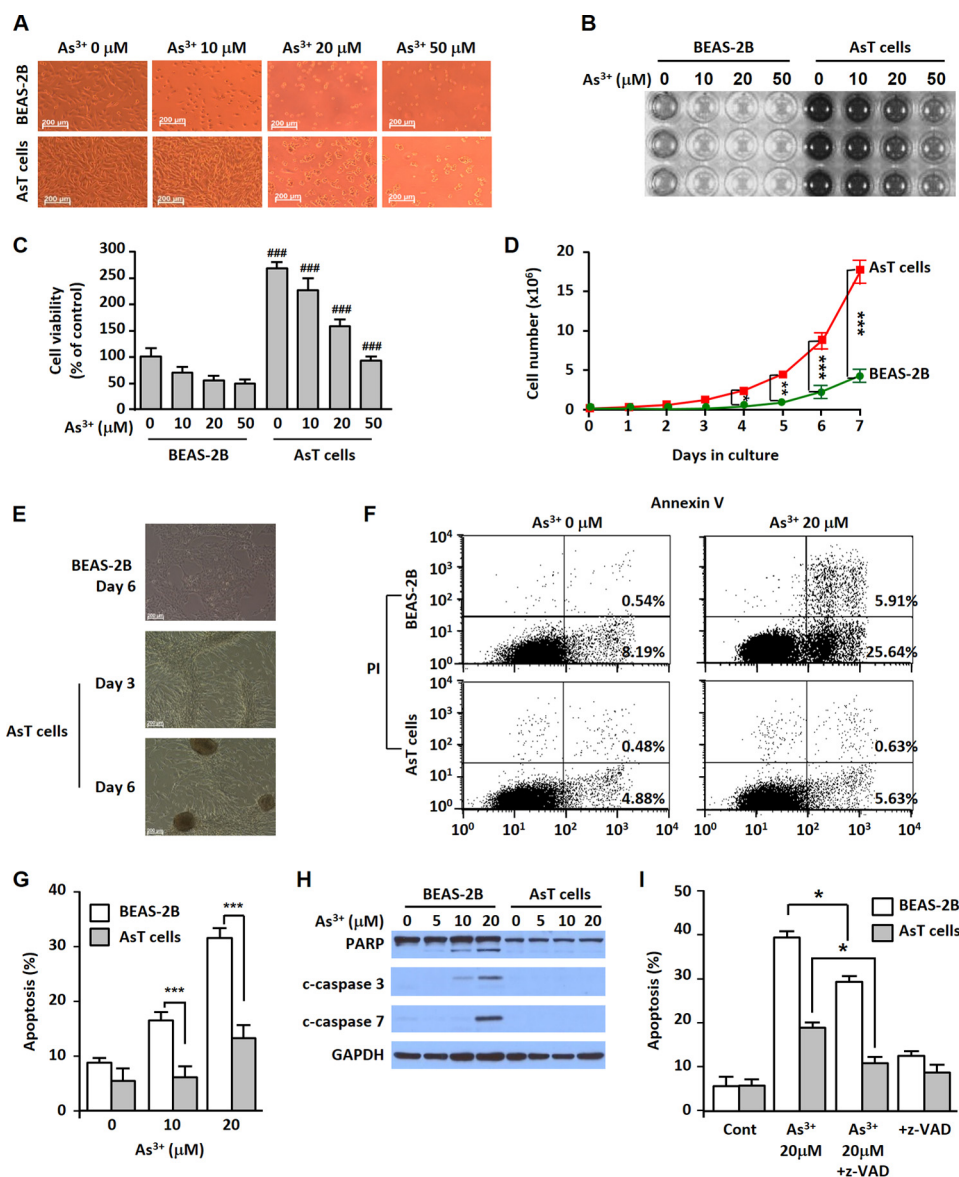
FIGURE 1. **AsT cells have cell death resistance, high proliferation, and tumorigenic potential.** AsT cells and their parent non-transformed BEAS-2B cells were exposed to increasing concentrations (0–50 μM) of As^{3+} for 24 h. The cell morphology was visualized by microscopy (*A*), and the 3-(4,5-dimethylthiazol-2yl-)-2,5-diphenyltetrazolium bromide assay results are presented by either photograph (*B*) or graph (*C*). The AsT cells and non-transformed cells (0.2 × 10^6) were seeded on 10-cm culture dishes for 7 days. The total cell number was counted each day (*D*). AsT and normal BEAS-2B cells (1 × 10^6) were seeded on 10-cm culture dishes. During culture periods, colony formation was observed (*E*). Cells were exposed to As^{3+} for 24 h, stained with annexin V and propidium iodide (*PI*), and then analyzed by a flow cytometer (*F* and *G*). The levels of poly(ADP-ribose) polymerase (*PARP*) and cleaved (*c*) caspase-3/7 were determined by Western blotting analysis (*H*). Cells were incubated with As^{3+} (20 μM) for 24 h in the presence and absence of the pancaspase inhibitor Z-VAD (20 μM) and an apoptosis assay was performed (*I*). *Cont*, control. The results are shown as the mean ± S.E. of triplicate or three independent experiments. ###, $p < 0.001$ *versus* the same concentration of arsenic-treated cells. *, $p < 0.05$; **, $p < 0.01$; and ***, $p < 0.001$ represent the significant differences between the experiments (ANOVA and Scheffé's test). *Error bars* represent S.E. GAPDH was used as a loading control. *Scale bars* in *A* and *E*, 200 μm.

transformed cells is similar to that of non-transformed cells (Fig. 2*L*).

Nrf2 and p62 Play a Critical Role for Cell Survival and Apoptosis Resistance of the AsT Cells—The basal levels of Nrf2 and p62 were higher in AsT cells than in non-transformed cells (Fig. 3, *A* and *F*). When normal cells were exposed to As^{3+}, the expression levels of Nrf2 and p62 were slightly increased. In AsT cells, the increased expression level was dramatic (Fig. 3, *B*, *C*, *G*, and *H*). The Nrf2 downstream target proteins NAD(P)H dehydrogenase, quinone 1 (NQO1) and HO-1 were elevated in the AsT cells (Fig. 3*C*). The Nrf2 negative regulator Keap1 was less expressed in AsT cells than in normal BEAS-2B cells (Fig. 3,

B and *C*). Moreover, the Keap1 expression level decreased by As^{3+} was restored after 12 h and started to increase in the BEAS-2B cells but not in the AsT cells (Fig. 3*C*). To further study the roles of Nrf2 and p62 in cell death resistance, we inhibited Nrf2 and p62 expressions by siRNA transfection (Fig. 3, *D* and *I*). The As^{3+}-mediated apoptosis was greatly accelerated by the blockage of Nrf2 or p62 expression in AsT cells (Fig. 3, *E* and *J*).

Nrf2 and p62 Cross-talk and As^{3+} Increase the Binding of Nrf2 to ARE Region of the p62/Bcl-2/Bcl-xL Promoter—After Nrf2 was knocked down, the basal level and increased level of Nrf2 by As^{3+} were abolished along with the p62 level (Fig.
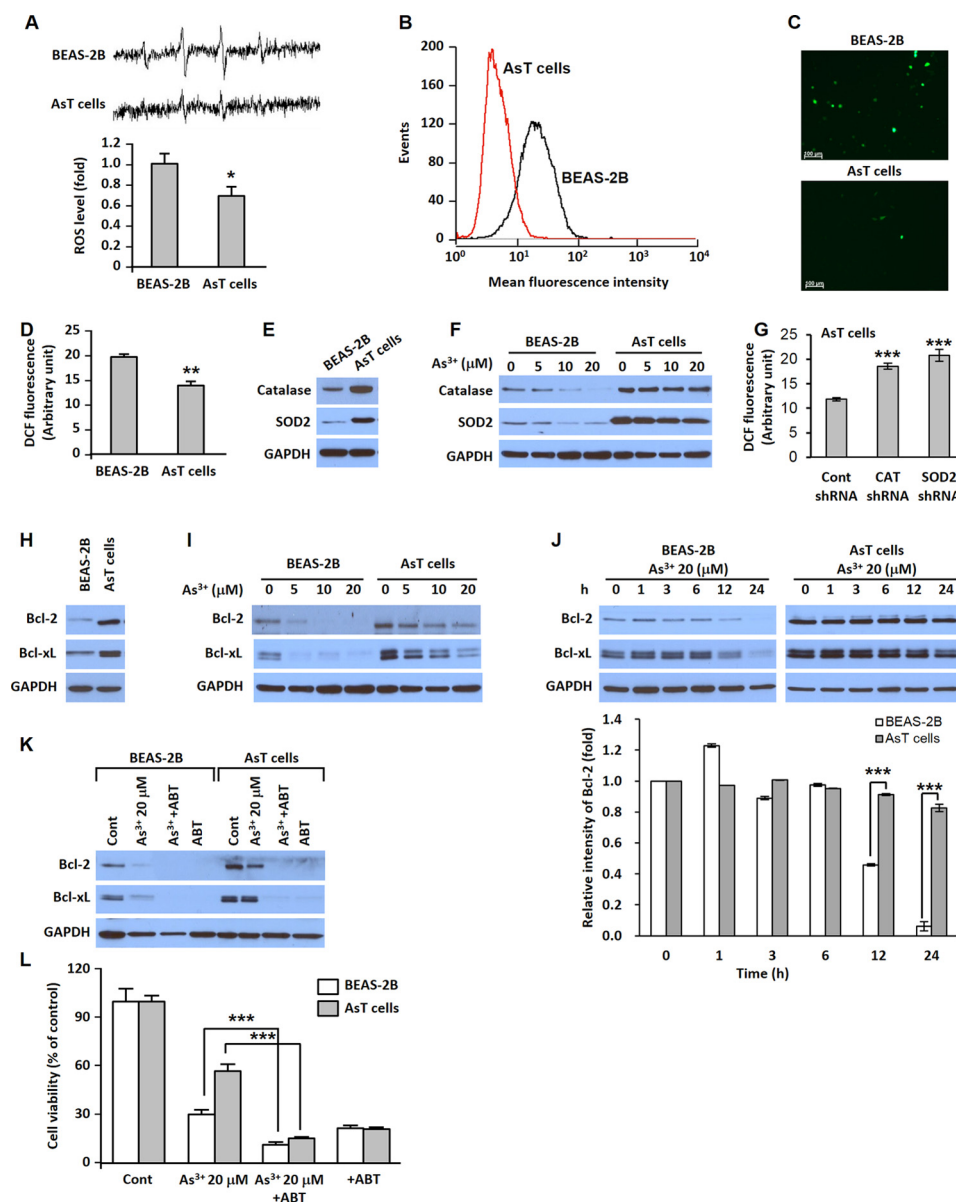
FIGURE 2. **AsT cells have a low level of ROS and highly express antioxidant enzymes and Bcl-2/Bcl-xL proteins.** The cell suspensions were prepared from AsT or normal cells, and then ESR spectra were recorded. The generation of a 1:2:2:1 quartet ESR signal is shown (*A*). ROS levels of the AsT cells and their parent BEAS-2B cells also were measured using flow cytometry (*B*), fluorescence microscopy (*C*), and a fluorescence microplate reader (*D*) after staining with 5-(and-6)-chloromethyl-2′,7′-dichlorodihydrofluorescein diacetate (*DCF*) (5 μM) for 30 min. The basal cellular levels of catalase (*CAT*), SOD2, Bcl-2, and Bcl-xL were measured (*E* and *H*). The ROS levels were measured after knockdown of catalase or SOD by shRNA transfection in the AsT cells (*G*). The effects of As^{3+} (0–20 μM) on the antioxidant enzymes and antiapoptotic proteins in the AsT cells or normal cells also were analyzed by Western blotting (*F*, *I*, and *J*). In addition, the quantification of Bcl-2 levels is represented (*J*, *lower panel*). For the inhibition assay, cells were incubated with As^{3+} (20 μM) for 24 h in the presence or absence of ABT-263 (*ABT*; 10 μM). Thereafter, the expression levels of Bcl-2 and Bcl-xL were detected (*K*), and cell viability was determined (*L*). The results are shown as the mean ± S.E. (*error bars*) of three separate experiments. *, $p < 0.05$ and **, $p < 0.01$ *versus* the normal BEAS-2B cells and ***, $p < 0.001$ represent a significant difference between the experiments (ANOVA and Scheffé's test). ABT-263 is a Bcl-2 family inhibitor. *Scale bars* in *C*, 100 μm. *Cont*, control.

4*A*). Furthermore, depletion of p62 reduced the basal level and As^{3+}-exposed normal and AsT cell p62 and Nrf2 levels (Fig. 4*A*). These results reveal that Nrf2 and p62 cross-talk with each other in the As^{3+}-exposed cells. The results of the ChIP assay demonstrate that Nrf2 binding to the ARE F5 (−493 to −481) in the p62 gene promoter was slightly increased in response to As^{3+} treatment in the normal BEAS-2B cells, whereas the binding was dramatically enhanced in AsT cells (Fig. 4, *B* and *C*). The decreased levels of Bcl-2/Bcl-xL expressions by As^{3+} and basal levels of Bcl-2/Bcl-xL were further accelerated by siRNA Nrf2 or p62 transfection in AsT cells (Fig. 4*D*, *lower panel*).

ChIP analysis revealed that Nrf2 binds to the ARE region of the Bcl-2 promoter (F1, −2991 to −2980) and that binding to the Bcl-xL promoter (F1, −2992 to −2984) increased in As^{3+}-exposed transformed cells (Fig. 4, *E* and *F*).

As^{3+}-transformed BEAS-2B Cells Have the Property of Autophagy Deficiency—When compared with normal cells, the expression levels of autophagy-related proteins such as ATG3, ATG5, and ATG7 were low in AsT cells without (Fig. 5*A*) and with As^{3+} treatment (Fig. 5*B*). As^{3+} treatment dramatically increased the LC3-II level in the normal cells, and LC3-II did not accumulate significantly in the AsT cells (Fig. 5*B*). Fluores-
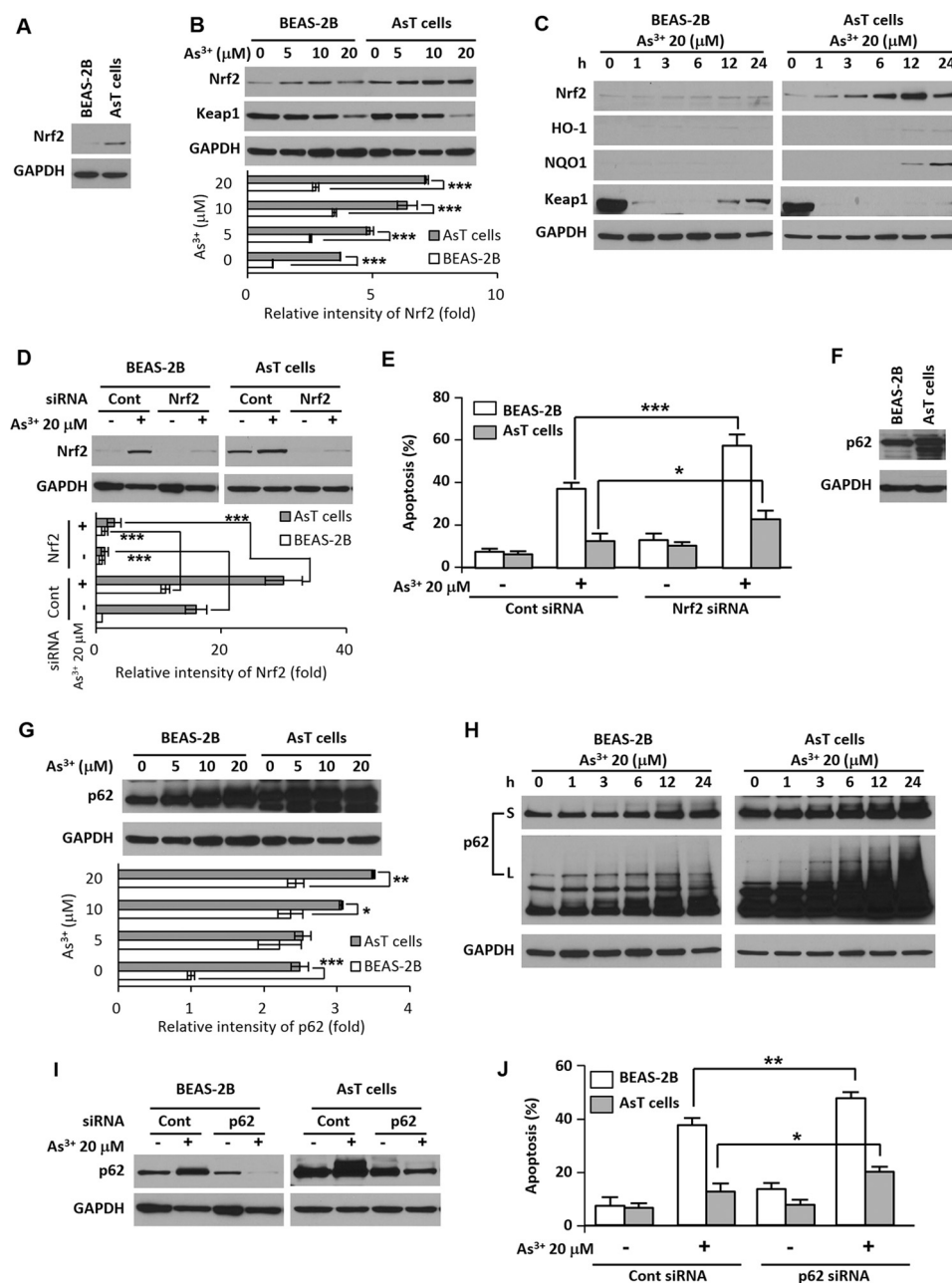
FIGURE 3. **Nrf2/p62 plays a critical role for cell survival and cell death resistance in the AsT cells.** The basal expression levels of Nrf2 and p62 were measured in the AsT cells and non-transformed BEAS-2B cells (*A* and *F*). The normal and AsT cells were exposed to various concentrations of As^{3+} (0–20 μM) for 24 h (*B* and *G*) or various times (0–24 h) with 20 μM As^{3+} (*C* and *H*), and then the levels of Nrf2, Keap1, p62, heme oxygenase-1 (*HO-1*), and NQO1 were detected. To diminish Nrf2 or p62 levels, cells were transfected with siRNA specific to Nrf2 or p62. After overnight transfection, cells were exposed to 20 μM As^{3+} for an additional 24 h (*D* and *I*), and an apoptosis assay was performed (*E* and *J*). The expression levels of Nrf2 or p62 were quantified and are represented in the *lower panels*. The results represent the mean $\pm$ S.E. (*error bars*) of three independent experiments. *, $p < 0.05$; **, $p < 0.01$; and ***, $p < 0.001$ represent a significant difference between the experiments (ANOVA and Scheffé's test). *S*, short exposure; *L*, long exposure; *Cont*, control.

cent puncta increased in both normal and transformed BEAS-2B cells when treated with As^{3+}, but significantly fewer puncta were observed in AsT cells (Fig. 5, *C* and *D*). Increased LC3-II levels were observed with bafilomycin A1 (an inhibitor of autophagosome and lysosome fusion) treatment in both BEAS-2B cells and transformed cells. LC3-II levels were further increased when treated with a combination of As^{3+} and bafilomycin A1, suggesting that As^{3+} increased autophagy flux rather than blocking the fusion of autophagosomes with lysosomes in BEAS-2B cells (Fig. 5, *E* and *F*). When the BEAS-2B

cells were treated with As^{3+} in the presence of wortmannin, an inhibitor of autophagosome initiation, the As^{3+}-induced upregulation of LC3-II was attenuated (Fig. 5, *E*, *bottom*, and *F*). To further study autophagy flux in the normal or transformed cells, we used tandem fluorescence-tagged LC3. When the transfected cells were exposed to As^{3+}, both yellow (mCherry$^+$/GFP$^+$) (autophagosome) and red (mCherry$^+$/GFP$^-$) (autolysosome) puncta were increased in normal BEAS-2B cells, whereas only yellow puncta with low intensity were increased in AsT cells (Fig. 5, *H* and *I*). Each image of
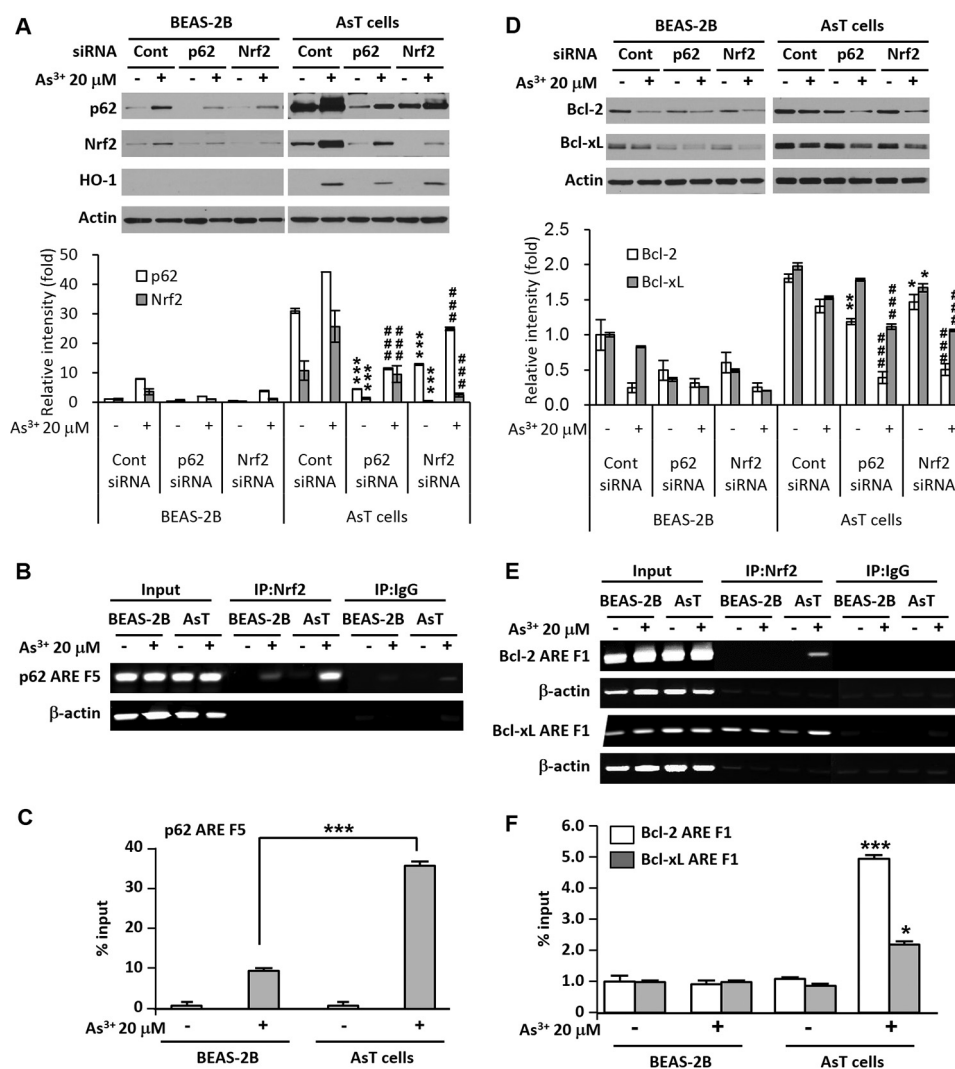
FIGURE 4. **Nrf2 and p62 have a positive feedback loop, and the binding activities of Nrf2 to the ARE regions of the p62, Bcl-2, and Bcl-xL promoters were increased in the arsenic-exposed AsT cells.** Cells were transfected with siRNA specific to p62 or Nrf2. After 12 h of transfection, the cells were treated with 20 μM As^{3+} for an additional 24 h. The expression levels of p62, Nrf2, heme oxygenase-1 (*HO-1*), and Bcl-2/Bcl-xL were analyzed (*A* and *D*). The expression levels of Nrf2/p62 and Bcl-2/Bcl-xL were quantified and are represented in *A* (*lower panel*) and *D* (*lower panel*), respectively. For the ChIP assay, cells were treated with As^{3+} (20 μM) for 6 h, fixed with formaldehyde, and cross-linked, and then chromatin was isolated. The chromatin was immunoprecipitated (*IP*) with an anti-Nrf2 antibody or control mouse IgG. The Nrf2 binding to the p62, Bcl-2, and Bcl-xL promoters was analyzed by normal real time PCR (*B* and *E*) or quantitative real time PCR (*C* and *F*) with a primer specific for the ARE region of the promoter. The data represent the percent input and are normalized to each control. The results are expressed as the mean $\pm$ S.E. (*error bars*) relative to the control of triplicate experiments. *, $p < 0.05$ and ***, $p < 0.001$ *versus* the untreated transformed control cells; ###, $p < 0.001$ *versus* the As^{3+}-treated transformed cells (ANOVA and Scheffé's test). Actin was used as a loading control. *Cont*, control.

GFP$^+$ and mCherry$^+$ is provided (Fig. 5*H*, *top* and *middle*). These results together with those in Fig. 5, *A–G*, indicate that autophagosomes were fused with lysosomes to generate autolysosomes in BEAS-2B cells but not in As^{3+}-transformed BEAS-2B cells. The relatively strong autophagy flux was induced by rapamycin alone, and As^{3+} exhibited some inhibition as shown by decreased levels of autophagosomes and autolysosomes (Fig. 5, *H* and *I*). These results show that As^{3+} is able to decrease the stress-activated autophagy flux in BEAS-2B cells. In transformed BEAS-2B cells, rapamycin alone induced autophagy flux at a lower level than that of normal BEAS-2B cells, showing that the transformed BEAS-2B cells indeed have some autophagy deficiency compared with their parent non-transformed BEAS-2B cells (Fig. 5, *H* and *I*). Similar to the results obtained using non-transformed cells, As^{3+} was able to decrease stress-induced autophagy flux in transformed

BEAS-2B cells. Taken together, the above autophagy flux results indicate that the autophagy process was uncompleted in the AsT cells. The expression levels of LC3-II in response to rapamycin and starvation condition (Fig. 5*G*) and lower level of ubiquitinated p62 (Fig. 5*J*) further confirmed autophagy deficiency in the AsT cells compared with the normal BEAS-2B cells. The results of the immunoprecipitation assay reveal that the high expression of Bcl-2 in the AsT cells may alter Beclin1 activity even though the Beclin1 expression levels were not different between these two types of cells (Fig. 5*K*). The results of the cell viability assay reveal that As^{3+}-induced autophagy was involved in the cell death mechanism rather than the cell survival mechanism because the autophagy activator rapamycin accelerated As^{3+}-induced cell death, whereas the autophagy inhibitor wortmannin attenuated it (Fig. 5*L*). Moreover, As^{3+}-induced apoptosis was significantly attenuated in autophagy-
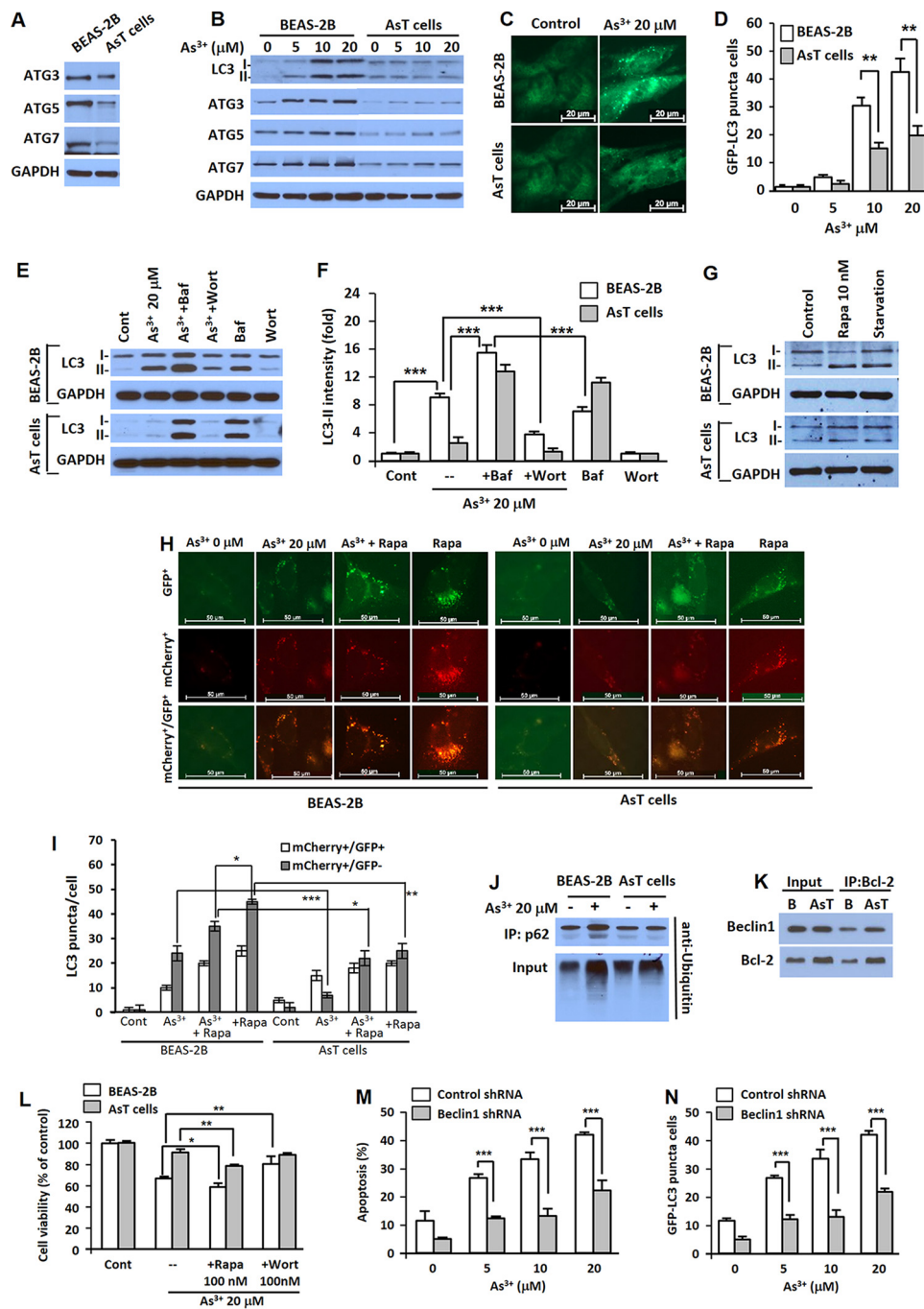
FIGURE 5. **AsT cells are characterized as having autophagy deficiency.** The basal expression level of autophagy-related proteins (ATG3, ATG5, and ATG7) were measured (*A*). Cells were exposed to various concentrations of As^{3+} (0–20 μM) for 24 h, and then the levels of LC3, ATG3, ATG5, and ATG7 were detected (*B*). The cells were transfected with the GFP-LC3 plasmid, treated with As^{3+}, and visualized (*C*), and the number of GFP-LC3 punctum-positive cells was counted (*D*). To analyze autophagy flux, the cells were preincubated with bafilomycin A1 (*Baf*) (100 nM) or wortmannin (*Wort*) (100 nM) for 1 h before treatment with As^{3+}. After 24-h incubation, the levels of LC3-I and LC3-II were detected (*E*). The expression level of LC3-II was quantified and is represented in *F*. The expression levels of LC3-I and LC3-II were further analyzed after exposure to rapamycin (10 nM) or in starvation condition (*G*) for further confirmation of autophagy deficiency of the AsT cells. The binding affinity of Bcl-2 with Beclin1 was analyzed by immunoprecipitation (*K*). The ubiquitination of p62 was further analyzed using anti-ubiquitin after performing immunoprecipitation (*IP*) (*J*). In addition, the cells were transfected with the mCherry-EGFP-LC3 plasmid and treated with As^{3+}. The *yellow* puncta (mCherry$^+$/GFP$^+$) and *red* puncta (mCherry$^+$/GFP$^-$) were visualized using fluorescence microscopy (*H*), and quantification of puncta is represented in *I*. For the inhibition assay, cells were incubated with As^{3+} (20 μM) for 24 h in the presence and absence of rapamycin (*Rapa*) (100 nM) or wortmannin (100 nM). Thereafter, cell viability was determined (*L*). The shRNA Beclin1-transfected stable BEAS-2B cells were treated with As^{3+} (0–20 μM) for 24 h, and the apoptotic cells (*M*) and fluorescent punctum-positive cells (*N*) were determined. The results are shown as the mean $\pm$ S.E. (*error bars*) in triplicate or three independent experiments. *, $p < 0.05$; **, $p < 0.01$; and ***, $p < 0.001$ represent a significant difference between the experiments (ANOVA and Scheffé's test). *Scale bars*, 20 (*C*) and 50 μm (*H*). *Cont*, control.

defective Beclin1 knockdown cells when compared with the vehicle control (Fig. 5*M*). This result corresponded to the GFP-LC3 punctum-positive cell population (Fig. 5*N*).

Nrf2 and p62 Regulate Intracellular ROS Levels, and ROS Is a Primary Initiator of Nrf2 and p62 Induction—The low basal levels of ROS were up-regulated in the siRNA p62- or in the
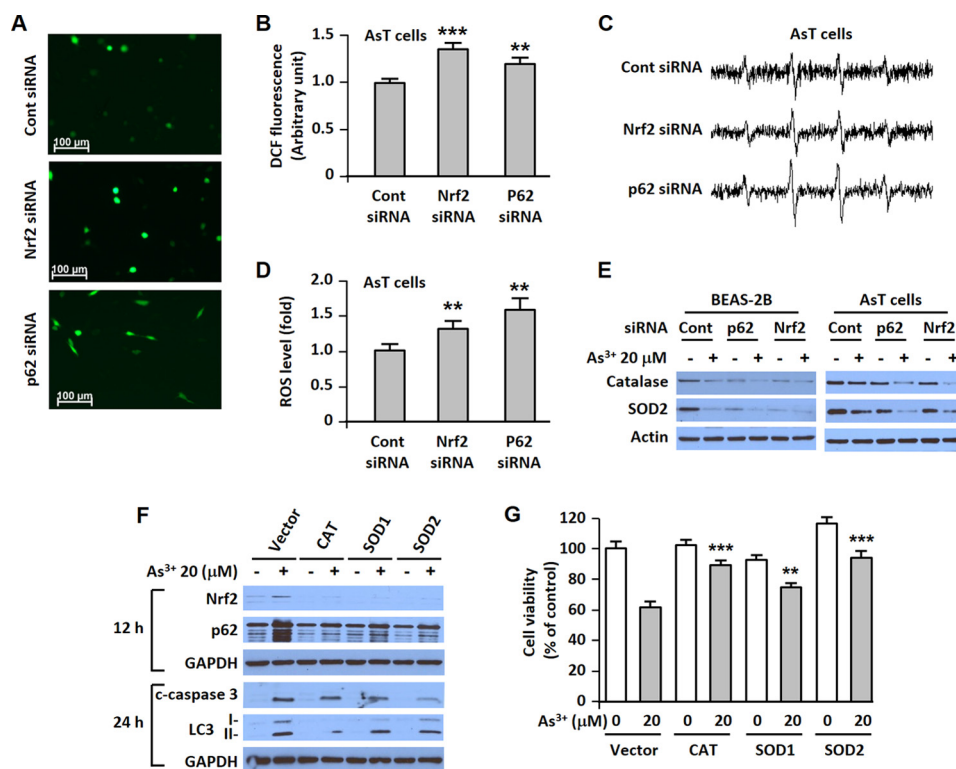
FIGURE 6. **Nrf2 and p62 regulate intracellular ROS levels.** ROS are a primary regulator of Nrf2 and p62 expression and the main mediator of apoptotic and autophagic cell death. AsT cells were transfected with siRNA specific to Nrf2 or p62. After overnight transfection, ROS levels were measured using fluorescence microscopy (*A*), a fluorescence microplate reader (*B*), and ESR (*C* and *D*). Cells were transfected with siRNA specific to p62 or Nrf2. After 12 h of transfection, the cells were exposed to 20 μM As^{3+} for an additional 24 h. The expression levels of catalase and SOD2 were measured (*E*). In addition, the catalase-, SOD1-, and SOD2-overexpressing stable BEAS-2B cells were exposed to As^{3+} (20 μM). The expression levels of p62, Nrf2, cleaved (*c*) caspase-3, and LC3 were analyzed (*F*), and then cell viability was determined (*G*). The results are shown as the mean ± S.E. (*error bars*) in triplicate experiments or three separate experiments. **, $p <$ 0.01 and ***, $p <$ 0.001 *versus* the unexposed BEAS-2B cells or the vehicle control (ANOVA and Scheffé's test). *Scale bars* in A, 100 μm. *CAT*, catalase; *Cont*, control; *DCF*, 5-(and-6)-chloromethyl-2',7'-dichlorodihydrofluorescein diacetate.

siRNA Nrf2-transfected transformed cells as shown by fluorescence microscopy (Fig. 6*A*), fluorometric assay (Fig. 6*B*), and ESR (Fig. 6, *C* and *D*). Furthermore, the expressions of antioxidant enzymes were further reduced in As^{3+}-exposed Nrf2 or p62 knockdown cells (Fig. 6*E*). The induction of Nrf2 or p62 by As^{3+} was attenuated with the endogenous overexpression of catalase, SOD1, or SOD2 (Fig. 6*F*). Our data revealed that the increased cleaved caspase-3 or LC3-II level was attenuated by endogenous overexpressed antioxidant enzymes (Fig. 6*F*). Moreover, As^{3+}-induced cell death was diminished by the depletion of ROS using endogenous antioxidant enzymes (Fig. 6*G*).

Role of Nrf2 in As^{3+}-induced Malignant Cell Transformation—Over the course of 6 months, BEAS-2B cells were exposed to As^{3+}, and colony numbers gradually increased (Fig. 7*A*). During the period of 2–3 months of exposure, As^{3+}-exposed shRNA Nrf2 or p62-transfected cells generated a higher level of colony numbers than 2–3-month As^{3+}-exposed vehicle control (Fig. 7*A*). However, at 4 months of As^{3+} exposure, cells with Nrf2 or p62 shRNA transfection exhibited less colony formation when compared with As^{3+}-exposed vehicle control during the same period (Fig. 7*A*). The inhibition effects on the colony formation by knockdown of Nrf2 or p62 were further enhanced at an exposure duration of 5 or 6 months (Fig. 7*A*). The xenograft assay also demonstrated that the tumor growth increased in the 2-month As^{3+}-exposed Nrf2 knockdown

BEAS-2B cells. The tumor growth was attenuated for 6-month As^{3+}-exposed Nrf2 knockdown cells compared with As^{3+}-exposed BEAS-2B cells used as a control (Fig. 7*B*). The growth of transformed cells on agar was dramatically inhibited by either Nrf2 shRNA or p62 shRNA transfection (Fig. 7*E*). The number of colonies was also attenuated by shRNA Nrf2- or p62-transfected AsT cells in the clonal assay (Fig. 7*F*).

The Expressions of Nrf2 and Its Related Proteins in Lung Adenocarcinoma—The expression levels of Nrf2, its downstream target protein NQO1, and p62 were dramatically increased in lung tumor tissues when compared with normal tissues from the same patients (Fig. 7*D*). However, the Keap1 expression levels were lower in all lung tumor tissues than in normal tissues (Fig. 7*D*). These results suggest that high expression of p62 along with down-regulation of Keap1 confers Nrf2 activation in lung adenocarcinoma. The antioxidant enzymes (catalase and SOD2) and antiapoptotic proteins (Bcl-2 and Bcl-xL) were highly expressed in lung tumor tissues (Fig. 7*D*). The high levels of expressions of Nrf2 and p62 in patient samples were further confirmed by immunohistochemistry (Fig. 7*C*). The malignance of tumor tissue was confirmed by ki67 and hematoxylin and eosin (H&E) staining (Fig. 7*C*).

Discussion

As^{3+} is a group I human carcinogen and ranks first on the Agency for Toxic Substance and Disease Registry 2013 Priority
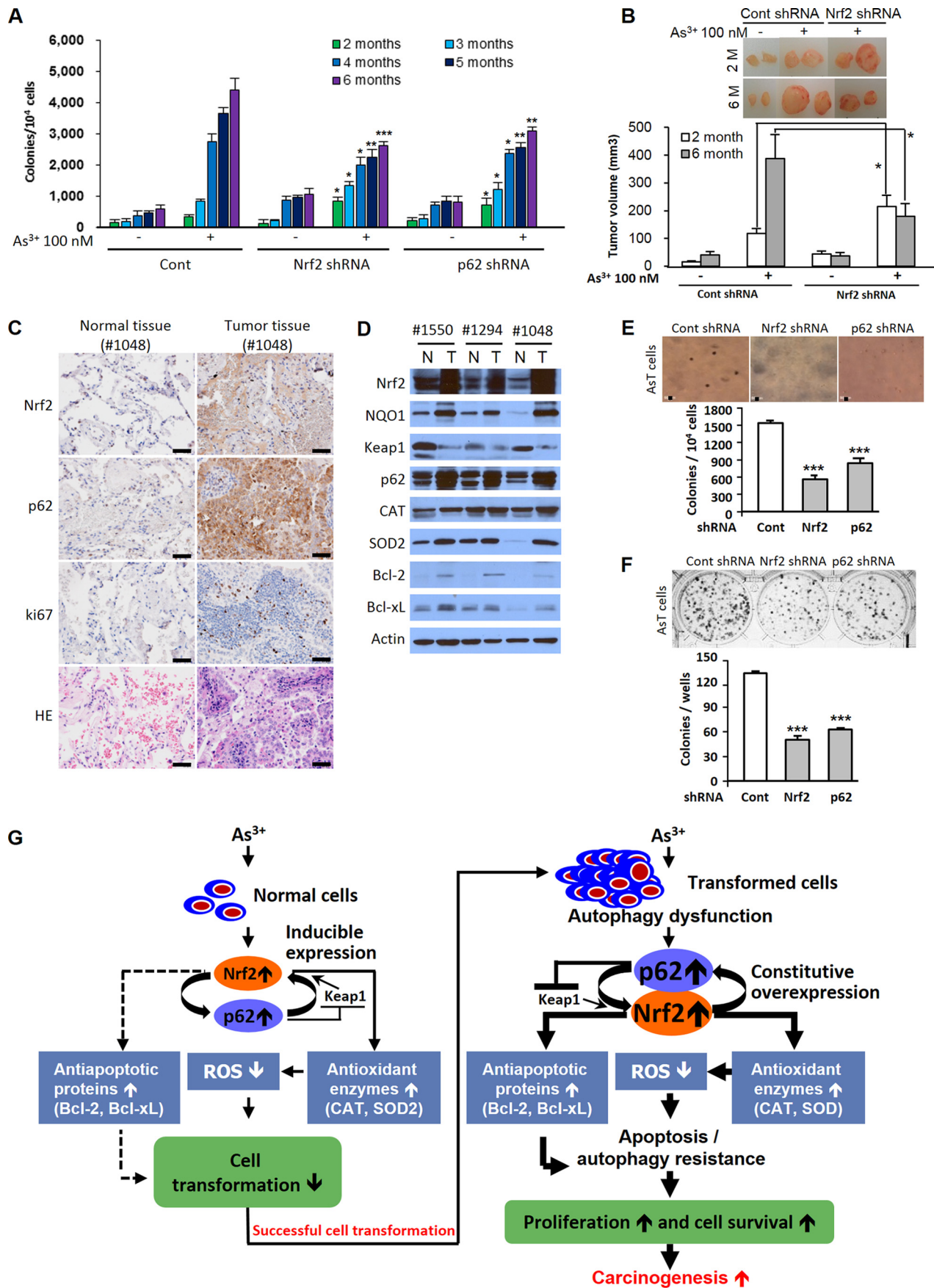
List of Hazardous Substances (19). Occupational or environmental exposure to As^{3+} induces lung cancer (20). Occupational As^{3+} exposure mainly occurs in mining, manufacturing, wood preservation, and agriculture (21). Cigarette smoke, As^{3+}-contaminated food, and As^{3+}-contaminated water are non-occupational sources of human exposure to As^{3+} (22). Our previous study has shown that chronic exposure of human bronchial epithelial cells to As^{3+} generates ROS and that ROS are responsible for As^{3+}-induced transformation of these cells (16). In our present study, we have shown that As^{3+}-transformed cells have a low level of ROS along with highly expressed antiapoptotic proteins (Bcl-2 and Bcl-xL) and antioxidant enzymes (catalase and SOD2) as well as Nrf2 and p62. We have also shown that As^{3+}-transformed cells have the properties of apoptosis resistance and autophagy dysfunction.

Most types of cancer cells show an apoptosis resistance and have a high proliferative potential (23). Our present study shows that AsT cells exhibit apoptosis resistance. The cell death resistance of AsT cells might be due to high expression of Bcl-2 and Bcl-xL based on the following results: 1) the basal levels of Bcl-2 and Bcl-xL are higher in AsT cells and 2) AsT cells show higher expression of Bcl-2/Bcl-xL than non-transformed cells when exposed to As^{3+} (Fig. 2, *H–L*). Another factor contributing to the apoptosis resistance is the low level of ROS in AsT cells. These cells carry a low level of ROS, making the cells less sensitive to As^{3+} toxicity (Fig. 2, *A–D*). Furthermore, higher expressions of antioxidant enzymes such as catalase and SOD2 help keep a low ROS concentration and contribute to cell death resistance in the AsT cells (Fig. 2, *E–G*) because knockdown of these antioxidant enzymes using shRNA in the AsT cells restored the low levels of ROS in these cells to the normal range (Fig. 2*G*). Nrf2 acts as a regulator of antioxidant and antiapoptotic proteins in As^{3+}-exposed cells (Figs. 6, *A–D*, and 3*E*). Nrf2 contributes to maintaining a low level of ROS due to up-regulation of catalase and SOD2 in the AsT cells (Fig. 6*E*). Nrf2 also activates the antiapoptotic proteins Bcl-2 and Bcl-xL in As^{3+}-exposed AsT cells (Fig. 4, *D–F*). The up-regulation of antiapoptotic proteins by Nrf2 might play a major role in apoptosis resistance in the As^{3+}-transformed cells.

Autophagy involves a cell death pathway, not a survival function, in our experimental setting because cell viability was enhanced by the addition of pharmacological inhibitors or the genetic depletion of autophagy in the As^{3+}-exposed normal BEAS-2B cells (Fig. 5, *L* and *M*). Moreover, cell viability is decreased by the addition of rapamycin, an autophagy activator (Fig. 5*L*). These results suggest that defective autophagy in the transformed cells has a beneficial effect for survival mechanisms. It has been reported that dysfunction of autophagy or defective autophagy causes up-regulation of p62 (24, 25). Our data show that AsT cells are characterized by autophagy deficiency (Fig. 5), which may result in the high expression of p62 in

transformed cells (Figs. 3*F* and 5). Notably, up-regulation of Bcl-2/Bcl-xL may further contribute to dysregulation of autophagy in the transformed cells as Bcl-2/Bcl-xL inhibits the autophagy function through the binding of the BH-3 domain of *Beclin1*, which is necessary for the induction of autophagy (26). Our findings also demonstrate that the binding of Bcl-2 with Beclin1 was higher in the AsT cells than in the normal BEAS-2B cells (Fig. 5*K*). Accumulation of p62 in transformed cells may contribute to apoptosis resistance and tumorigenesis (Figs. 3, *F–J*, and 7) through down-regulation of ROS generation (Fig. 6, *A–E*). Depletion of p62 by siRNA transfection resulted in a decrease of As^{3+}-induced Nrf2 expression in transformed cells (Fig. 4*A*). Knockdown of Nrf2 by siRNA transfection also attenuated As^{3+}-induced p62 expression in the AsT cells (Fig. 4*A*). These results indicate a possible positive feedback loop between Nrf2 and p62 in the transformed cells. Furthermore, Nrf2 binding activities on p62 promoter were dramatically enhanced in the transformed cells upon exposure to As^{3+} (Fig. 4, *B* and *C*). This might be the main reason for the increase of p62 levels during As^{3+} exposure periods in the cells (Fig. 3, *G* and *H*). It is notable that the basal high level of p62 in the transformed cells is not a direct cause of Nrf2 activation because activation of Nrf2 binding to the ARE region of the p62 promoter was not higher in the non-stimulated AsT cells than in the normal cells (Fig. 4, *B* and *C*). Presumably, high expression of p62 is mainly due to autophagy deficiency in the transformed cells.

The expression of Nrf2 or p62 was markedly higher in the lung adenocarcinoma tissues than in normal tissues from the same patients (Fig. 7, *C* and *D*). Furthermore, other Nrf2 regulator proteins such as antioxidant enzymes (catalase and SOD2) and antiapoptotic proteins (Bcl-2 and Bcl-xL) along with Nrf2 downstream target protein NQO1 were highly expressed in lung adenocarcinoma tissues (Fig. 7*D*). These results support the pathological significance of Nrf2 and p62 signaling in human lung cancer. However, Nrf2 has a protective role in cell transformation during premalignant stages because As^{3+}-induced cell transformation was further enhanced by knockdown of Nrf2 by shRNA transfection after 2 or 3 months of exposure (Fig. 7, *A* and *B*). It is likely that inducible Nrf2 is antioncogenic due to up-regulation of antioxidants to reduce the levels of ROS, leading to decreased cell transformation. The protective function of Nrf2 in the cells against cell transformation might be lost when the cells are exposed to As^{3+} continually. Furthermore, the protective role of Nrf2 in cell transformation is reversed after 4 months of As^{3+} exposure (Fig. 7, *A* and *B*). At this stage, the constitutive activation of Nrf2 may promote cell survival and increase cell proliferation by induction of apoptosis resistance of genetically damaged cells. These results suggest that Nrf2 has an antioncogenic or oncogenic role depending on the stage of cell transformation. Overall, this study demon-

FIGURE 7. Antioncogenic or oncogenic role of Nrf2 and its critical role in lung adenocarcinoma development. BEASE-2B cells in which Nrf2 or p62 was knocked down with shRNA transfection were exposed to 100 nM As^{3+} for 6 months, and soft agar (*A*) and xenograft assays (*B*) were performed. AsT cells were transfected with shRNA specific for either Nrf2 or p62, and then a soft agar assay (*E*) and clonal assay (*F*) were performed. Human lung adenocarcinoma tissues (stage IA or IIA) were homogenized, and Western blotting analysis (*D*) or immunohistochemical staining (*C*) was performed. The results are shown as the mean ± S.E. (*error bars*) in three independent experiments. *, $p < 0.05$; **, $p < 0.01$; ***, $p < 0.001$ *versus* the As^{3+}-exposed vehicle control or the untreated vehicle control cells (ANOVA and Scheffé's test). Actin was used as an internal control. 1550, stage IIA; 1294, stage IIA; 1048, stage IA. *G*, scheme showing the dual role of Nrf2 in As^{3+}-exposed human bronchial epithelial cells. S*cale bars* in *C* and *E*, 50 μm. *CAT*, catalase; *Cont*, control; *N*, normal; *T*, tumor.

strates the integration of Nrf2, p62, ROS, autophagy, apoptosis, and cell survival in As^{3+}-induced carcinogenesis (Fig. 7*G*). As^{3+}-induced ROS have been shown to have oncogenic properties in the premalignant stage; exposure of human lung bronchial epithelial cells to As^{3+} generates ROS, which are responsible for malignant transformation of these cells (16). In this stage, the Nrf2 is inducible and is regulated by Keap1. By upregulating antioxidant enzymes to reduce ROS, this very well regulated protein has an antioncogenic property. Notably, the up-regulation of antiapoptotic proteins by Nrf2 is negligible in the premalignant stage. After transformation (*e.g.* the postmalignant stage), ROS play an antioncogenic role. A low level of ROS increases survival and proliferation of transformed cells and tumorigenesis. In this stage, constitutive overexpression of Nrf2 has an oncogenic property. This protein is mainly regulated by p62 rather than Keap1. Its inducible property is lost. The constitutive overexpression of Nrf2 further up-regulates antioxidant enzymes and antiapoptotic proteins in the transformed cells. These phenomenon cause low cellular ROS levels and the acquisition of apoptosis resistance. Furthermore, high expression of p62 due to defective autophagy leads to accelerated Nrf2 activation. This process promotes cell survival, proliferation, and carcinogenesis of transformed cells. Our findings provide a potential chemoprevention and chemotherapy strategy for metal-induced carcinogenesis through manipulation of Nrf2 expression and activity.

References

1. Edwards, M. R., Johnson, B., Mire, C. E., Xu, W., Shabman, R. S., Speller, L. N., Leung, D. W., Geisbert, T. W., Amarasinghe, G. K., and Basler, C. F. (2014) The Marburg virus VP24 protein interacts with Keap1 to activate the cytoprotective antioxidant response pathway. *Cell Rep.* **6,** 1017–1025
2. Nezis, I. P., and Stenmark, H. (2012) p62 at the interface of autophagy, oxidative stress signaling, and cancer. *Antioxid. Redox Signal.* **17,** 786–793
3. Duran, A., Linares, J. F., Galvez, A. S., Wikenheiser, K., Flores, J. M., Diaz-Meco, M. T., and Moscat, J. (2008) The signaling adaptor p62 is an important NF-κB mediator in tumorigenesis. *Cancer Cell* **13,** 343–354
4. Lau, A., Zheng, Y., Tao, S., Wang, H., Whitman, S. A., White, E., and Zhang, D. D. (2013) Arsenic inhibits autophagic flux, activating the Nrf2-Keap1 pathway in a p62-dependent manner. *Mol. Cell. Biol.* **33,** 2436–2446
5. Komatsu, M., Kurokawa, H., Waguri, S., Taguchi, K., Kobayashi, A., Ichimura, Y., Sou, Y. S., Ueno, I., Sakamoto, A., Tong, K. I., Kim, M., Nishito, Y., Iemura, S., Natsume, T., Ueno, T., Kominami, E., Motohashi, H., Tanaka, K., and Yamamoto, M. (2010) The selective autophagy substrate p62 activates the stress responsive transcription factor Nrf2 through inactivation of Keap1. *Nat. Cell Biol.* **12,** 213–223
6. Jain, A., Lamark, T., Sjøttem, E., Larsen, K. B., Awuh, J. A., Øvervatn, A., McMahon, M., Hayes, J. D., and Johansen, T. (2010) p62/SQSTM1 is a target gene for transcription factor NRF2 and creates a positive feedback loop by inducing antioxidant response element-driven gene transcription. *J. Biol. Chem.* **285,** 22576–22591
7. Adams, J. M., and Cory, S. (2007) The Bcl-2 apoptotic switch in cancer development and therapy. *Oncogene* **26,** 1324–1337
8. Junttila, M. R., and Evan, G. I. (2009) p53—a Jack of all trades but master of none. *Nat. Rev. Cancer* **9,** 821–829
9. Hanahan, D., and Weinberg, R. A. (2011) Hallmarks of cancer: the next generation. *Cell* **144,** 646–674
10. White, E., and DiPaola, R. S. (2009) The double-edged sword of autophagy modulation in cancer. *Clin. Cancer Res.* **15,** 5308–5316
11. Levine, B., and Kroemer, G. (2008) Autophagy in the pathogenesis of disease. *Cell* **132,** 27–42
12. Sporn, M. B., and Liby, K. T. (2012) NRF2 and cancer: the good, the bad and the importance of context. *Nat. Rev. Cancer* **12,** 564–571
13. Hayes, J. D., McMahon, M., Chowdhry, S., and Dinkova-Kostova, A. T. (2010) Cancer chemoprevention mechanisms mediated through the Keap1-Nrf2 pathway. *Antioxid. Redox Signal.* **13,** 1713–1748
14. Hu, R., Saw, C. L., Yu, R., and Kong, A. N. (2010) Regulation of NF-E2-related factor 2 signaling for cancer chemoprevention: antioxidant coupled with antiinflammatory. *Antioxid. Redox Signa.* **13,** 1679–1698
15. Wang, X. J., Sun, Z., Villeneuve, N. F., Zhang, S., Zhao, F., Li, Y., Chen, W., Yi, X., Zheng, W., Wondrak, G. T., Wong, P. K., and Zhang, D. D. (2008) Nrf2 enhances resistance of cancer cells to chemotherapeutic drugs, the dark side of Nrf2. *Carcinogenesis* **29,** 1235–1243
16. Chang, Q., Pan, J., Wang, X., Zhang, Z., Chen, F., and Shi, X. (2010) Reduced reactive oxygen species-generating capacity contributes to the enhanced cell growth of arsenic-transformed epithelial cells. *Cancer Res.* **70,** 5127–5135
17. Son, Y. O., Wang, L., Poyil, P., Budhraja, A., Hitron, J. A., Zhang, Z., Lee, J. C., and Shi, X. (2012) Cadmium induces carcinogenesis in BEAS-2B cells through ROS-dependent activation of PI3K/AKT/GSK-3β/β-catenin signaling. *Toxicol. Appl. Pharmacol.* **264,** 153–160
18. Son, Y. O., Wang, X., Hitron, J. A., Zhang, Z., Cheng, S., Budhraja, A., Ding, S., Lee, J. C., and Shi, X. (2011) Cadmium induces autophagy through ROS-dependent activation of the LKB1-AMPK signaling in skin epidermal cells. *Toxicol. Appl. Pharmacol.* **255,** 287–296
19. Agency for Toxic Substances and Disease Registry (2013) *Priority List of Hazardous Substances*, Agency for Toxic Substances and Disease Registry, Atlanta, GA
20. Bode, A. M., and Dong, Z. (2002) The paradox of arsenic: molecular mechanisms of cell transformation and chemotherapeutic effects. *Crit. Rev. Oncol. Hematol.* **42,** 5–24
21. Wickre, J. B., Folt, C. L., Sturup, S., and Karagas, M. R. (2004) Environmental exposure and fingernail analysis of arsenic and mercury in children and adults in a Nicaraguan gold mining community. *Arch. Environ. Health* **59,** 400–409
22. Hughes, M. F. (2002) Arsenic toxicity and potential mechanisms of action. *Toxicol. Lett.* **133,** 1–16
23. Hanahan, D., and Weinberg, R. A. (2000) The hallmarks of cancer. *Cell* **100,** 57–70
24. Mathew, R., Karp, C. M., Beaudoin, B., Vuong, N., Chen, G., Chen, H. Y., Bray, K., Reddy, A., Bhanot, G., Gelinas, C., Dipaola, R. S., Karantza-Wadsworth, V., and White, E. (2009) Autophagy suppresses tumorigenesis through elimination of p62. *Cell* **137,** 1062–1075
25. Lau, A., Wang, X. J., Zhao, F., Villeneuve, N. F., Wu, T., Jiang, T., Sun, Z., White, E., and Zhang, D. D. (2010) A noncanonical mechanism of Nrf2 activation by autophagy deficiency: direct interaction between Keap1 and p62. *Mol. Cell. Biol.* **30,** 3275–3285
26. Maiuri, M. C., Zalckvar, E., Kimchi, A., and Kroemer, G. (2007) Self-eating and self-killing: crosstalk between autophagy and apoptosis. *Nat. Rev. Mol. Cell Biol.* **8,** 741–752

Antioncogenic and Oncogenic Properties of Nrf2 in Arsenic-induced Carcinogenesis

Young-Ok Son, Poyil Pratheeshkumar, Ram Vinod Roy, John Andrew Hitron, Lei Wang, Sasidharan Padmaja Divya, Mei Xu, Jia Luo, Gang Chen, Zhuo Zhang and Xianglin Shi

Access the most updated version of this article at doi: 10.1074/jbc.M115.675371

Alerts:
- When this article is cited
- When a correction for this article is posted

Click here to choose from all of JBC's e-mail alerts

This article cites 25 references, 6 of which can be accessed free at
http://www.jbc.org/content/290/45/27090.full.html#ref-list-1